

# Nanoscale Advances

Accepted Manuscript

This article can be cited before page numbers have been issued, to do this please use: B. Ocampo Cardenas, G. Román, E. Nosedá Grau and S. Simonetti, *Nanoscale Adv.*, 2025, DOI: 10.1039/D4NA00776J.



This is an Accepted Manuscript, which has been through the Royal Society of Chemistry peer review process and has been accepted for publication.

Accepted Manuscripts are published online shortly after acceptance, before technical editing, formatting and proof reading. Using this free service, authors can make their results available to the community, in citable form, before we publish the edited article. We will replace this Accepted Manuscript with the edited and formatted Advance Article as soon as it is available.

You can find more information about Accepted Manuscripts in the [Information for Authors](#).

Please note that technical editing may introduce minor changes to the text and/or graphics, which may alter content. The journal's standard [Terms & Conditions](#) and the [Ethical guidelines](#) still apply. In no event shall the Royal Society of Chemistry be held responsible for any errors or omissions in this Accepted Manuscript or any consequences arising from the use of any information it contains.

# Study of clopidogrel and clonidine interactions for cardiovascular

View Article Online

DOI: 10.1039/D4NA00776J

## formulation: Progress from DFT modeling

B. Ocampo Cárdenas<sup>1</sup>, G. Román<sup>2,3</sup>, E. Noseda Grau<sup>2,3</sup>, S. Simonetti<sup>2,3</sup>

<sup>1</sup>Universidad del Quindío, Carrera 15 con calle 12 norte, Armenia, Quindío, Colombia

<sup>2</sup>Universidad Tecnológica Nacional, Facultad Regional Bahía Blanca, 11 de Abril 461, (B8000LMI) Bahía Blanca, Buenos Aires, Argentina.

<sup>3</sup>Instituto de Física del Sur (IFISUR), Departamento de Física, Universidad Nacional del Sur (UNS), CONICET, Av. L. N. Alem 1253, B8000CPB - Bahía Blanca, Argentina.

e-mail: BOCAMPOC@uqvirtual.edu.co

### Abstract

Clopidogrel and clonidine drugs are frequently used to treat cardiovascular illnesses which are the leading cause of mortality worldwide. Since these medications are frequently taken in combination, it is crucial to examine their molecular interactions. Therefore, the band-gap energy, chemical potential, chemical hardness and softness parameters are calculated by Density Functional Theory (DFT) based method. In addition, Infrared (IR) spectrum, Natural Bond Orbital (NBO), molecular electrostatic potential (MEP), Electron Localization Function (ELF) and Total Density of States (TDOS) plots complement the analysis.

Clonidine presents greater sensitivity to electrophilic attack, while, the electronic affinity is little higher for clopidogrel. Negative charge density is located in oxygen atoms of clopidogrel and positive charge is placed in nitrogens of clonidine, according to MEP map. On the other hand, the drugs present similar reactivity in water. Clopidogrel is lesser reactive than clonidine, and the interaction between the molecules is taken place by physisorption, in agreement with TDOS plot. NBO analysis reveals a low charge variation in accordance with the physical adsorption-like bonding between the drugs. The lowest energy for clopidogrel-clonidine interaction is reached by the formation of four H bonds that is observed in IR spectrum by a significant intensity peak at 3360 cm<sup>-1</sup>. Hydrogen-bonds play a crucial role for controlled drug delivery application as it allows moderate and reversible drug adsorption, facilitating its release in the biological environment. IR spectra also support the absence of degradation or chemical reaction between the drugs confirming the preservation of the active pharmaceutical individual ingredient.

**Keywords:** drug delivery; clopidogrel, clonidine, DFT



## 1. Introduction

View Article Online  
DOI: 10.1039/D4NA00776J

Cardiovascular diseases (CVDs) are the leading cause of mortality globally, registering 20.5 million CVD-related deaths in 2021 [1]. Cardiovascular medicines, as clopidogrel and clonidine drugs, are critical for the prevention and management of CVD drugs for long term treatment of patients.

Clopidogrel (Fig. 1 (a)) is an analogue of ticlopidine [2]. Its chemical structure is methylalpha-(2-chlorophenyl)-6,7-dihydrothieno[3,2-c]pyridine-5(4H)acetate.

Clopidogrel is a prodrug that has pharmacological activity; since antiplatelet activity is dependent on its hepatic transformation into a thiol metabolite through oxidation and hydrolysis. In the coagulation mechanism, platelets adhere to the sub endothelium that has been exposed afterward tissue injury. After this first phase of adhesion, platelets join other platelets in the process called aggregation, through which the thrombus is formed. The platelet receptor, GPIIb-IIIa [3], actively participates in both processes. Clopidogrel blocks [4] the platelet adenosine diphosphate (ADP) receptor [5]. In this way, the binding of fibrinogen to the receptor, the GPIIb-IIIa glycoprotein [6], is inhibited preventing the continuity of aggregation cascade. Clopidogrel acts reducing the fibrinogen-GPIIb-IIIa binding without altering this complex [7]. The platelet modification caused by clopidogrel active metabolite is irreversible [8]. In 2022, clopidogrel was ranked 47<sup>th</sup> in the top 200 prescribed medication in the United States [9]. Due the importance of clopidogrel in the actual pharmaceutical industry, many articles have been recently publicized. Forced degradation studies have been the object of interest by the scientific community and pharmaceutical industries, in order to investigate the intrinsic stability of clopidogrel under various stress conditions [10, 11]. A study shows that patients at extreme CVD risk has more genetic resistance to clopidogrel [12]. These patients have more coronary events; therefore, it should study the genetic resistance to individualize antiplatelet



treatment. On the other hand, Raman spectra simulation was obtained from the interaction of clopidogrel metabolite with P2Y<sub>12</sub> receptor [13]. The theoretical data were compared with the experimental SERS results. The prospects of obtaining results for pathologies based on platelet conformations during cardiovascular diseases have been successfully demonstrated [13].

Clonidine (Fig. 1 (a)), the imidazole alpha-2-adrenergic agonist, was introduced into clinical practice, firstly, as a nasal decongestant, but its systemic effects were rapidly known, such as arterial hypotension, bradycardia and sedation [14]. Once the hypotensive effect of clonidine in the central and peripheral nervous systems was demonstrated, it began to be prescribed for the control of high blood pressure. In recent decades, the advantages of clonidine were recognized and its use also spread in the field of anesthesia in cardiac surgery. Among other benefits, the reduction of opioid administration in the intra- and postoperative periods was attributed to clonidine, which allows rapid tracheal extubation and short period of mechanical ventilation. The cardiovascular action of clonidine is well known. Its vasodilatory activity is due to peripheral and central mechanisms that leads to a reduction in blood pressure [15-17]. In 2022, clonidine was ranked 71<sup>th</sup> in the top 200 prescribed medication in the United States [9]. Owing the importance of clonidine in the actual pharmaceutical industry, from past years to the actually, many articles have been publicized. Experimental and theoretical approaches were combined to investigate the thermodynamics and kinetics characteristics of clonidine oxidation in remedial studies [18]. On the other hand, structural properties and FTIR-Raman spectra of the clonidine hydrochloride and their dimeric species were determined [19]. The knowledge of the structures and vibrational properties of these anti-hypertensive agents are essential for their quick identifications, for the synthesis of new derivatives with improved pharmacologic properties and, to know and explain their



behaviors and mode of action [19]. The effects of clonidine on the cardiovascular, renal and inflammatory responses to experimental bacteremia were also studied [20]. High clinical dose of clonidine attenuated sepsis-related increases in heart rate and cardiac output, with little effect on arterial pressure. It also induced a water diuresis, reduced body temperature, and had an anti-inflammatory action. Low-dose clonidine had similar but less pronounced effects, except that it induces moderate vasodilatation and increases cardiac output. A study was done to reveal the benefit of clonidine as an adjuvant therapy to bupivacaine [21]. Low doses of clonidine along with bupivacaine show no side effects, and well-maintained systolic blood pressure with analgesia for longer period of time.

In recent years, an increase interest in artificial intelligence and computational methods has been observed [22]. Valuable Density Functional Theory (DFT) based works in the field of interaction of different molecules with various substrates have been recent publicized [23-33]. Using DFT calculations, the adsorptions of SO<sub>2</sub>, SO<sub>3</sub> and O<sub>3</sub> gas molecules on MoS<sub>2</sub> monolayers were studied in terms of adsorption energy, charge transfer, band structures, and charge density differences [23]. Various adsorption geometries and sites were considered in detail for the adsorption behaviors of SO<sub>x</sub> molecules on the pristine and N-doped ZnO nanoparticles using DFT calculations [24]. Theoretical investigation of CO and NO gas molecules shows shorter adsorption distance and higher adsorption energy for Al-doped and Si-doped monolayers than the P-doped and pristine ones [25]. Charge density difference calculations show the charge accumulation between the interacting atoms, suggesting the formation of covalent bonds, as evidenced by the projected density of states of the interacting atoms [25]. DFT study of the adsorption of O<sub>3</sub> and NO<sub>2</sub> molecules on ZnO nanoparticles provides a theoretical basis, giving rise to design of innovative and highly efficient sensor devices [26]. Theoretical findings show that TiO<sub>2</sub>/Stanene heterostructure holds great promise for



fabricating novel and highly sensitive NO<sub>2</sub> and O<sub>3</sub> gas sensors [28]. The interaction of gas molecules (CO, NO, N<sub>2</sub>O and NH<sub>3</sub>) with Pd decorated stanene nanosheets was studied using DFT calculations [29]. The considerable electron orbital overlaps between gas molecules and Pd-embedded stanene confirm that strong chemisorption occurs showing great potential as promising candidate for gas sensing [29].

Cardiac diseases are one of the principal causes of death worldwide. In these situations, patients receive multifaceted pharmacological pills that result in a low adherence rate. The combination of drugs has been shown in clinical studies to increase the antihypertensive efficacy of both agents compared to either agent alone [34]. Consequently, a formulation containing clonidine and clopidogrel drugs, for cardiovascular treatment could improve administration in patients. In this contest, it is crucial to study the drug properties and the drug-drug interactions in their chemical environment. The objective of this research is to lead to a more complete understanding of the physical phenomena that could occur in this multi-drug system. This work emphasizes the role of computational chemistry as a clean technique in analyze the drug-drug interactions, paving the way for future experimental research in this field.

## 2. Theoretical method

The isolated molecules and configurations have been modeled with GaussView05 [35] and all calculations were done using the Gaussian 09 package [36]. Full geometry optimizations have been performed using Density Functional Theory (DFT) with a correlation functional of Lee, Yang, Parr (B3LYP) level using 6-31G basis set [37-39]. Dispersion effects are incorporated by the correction based Grimme's (D3) approach [40]. We highlight the efficacy of the functional and basis set used in this study. B3LYP is a commonly used functional in a variety of systems, while 6-31G basis set is suitable used



for general calculations on medium to huge molecules and it is an optimal level of theory to deliver reliable results at minimum cost [40-43]. Real biological environments are mimicked by optimizing all the studied structures in the water solvent. Solvent effects are incorporated in calculations using the polarizable continuum model [44] that is a continuum solvent model already well-developed and widely used in treating solvent effects on molecular properties [45] due the reliability of the model [46].

There is a strong relationship between quantum chemical parameters linked to the electronic structure and the chemical behavior of molecules during interactions [47, 48]. Chemical parameters can be calculated when molecular orbitals, such as the HOMO (Highest Occupied Molecular Orbital) and the LUMO (Lowest Occupied Molecular Orbital) are available [49]. From the frontier orbitals, we can determine the energy band gap, defined as,

$$E_g = (E_{LUMO} - E_{HOMO}) \quad (1)$$

which indicates the activity of the molecule in chemical reactions. From the band gap, we can define a series of parameters.

We can describe the hardness “ $\eta$ ” as,

$$\eta = (E_{LUMO} - E_{HOMO})/2 \quad (2)$$

Hardness is defined as the measure of the resistance to deformation of the chemical structure in an external electric field. The increase in hardness implies more stability. On the contrary, if the gap is small, it can describe by the global softness (S),

$$S = 1/(2\eta) \quad (3)$$

which is the reciprocal of hardness.

Another descriptor is the electronic chemical potential ( $\mu$ ),

$$\mu = (E_{HOMO} + E_{LUMO})/2 \quad (4)$$

which is associated with the ability of the molecule to exchange electron density.



Different interaction mechanisms between the drugs are involved in the systems, View Article Online  
DOI: 10.1039/D4NA00776J

therefore, we can define the electrophilicity ( $\omega$ ) as,

$$\omega = \mu^2 / 2\eta \quad (5)$$

which measures the change in the energy of an electrophile specie when it becomes saturated with electrons.

The different clopidogrel-clonidine configurations were optimized and we have calculated the adsorption energy ( $\Delta E$ ) as,

$$\Delta E = E_{\text{clopidogrel-clonidine}} - (E_{\text{clopidogrel}} + E_{\text{clonidine}}) \quad (6)$$

The positive value of  $\Delta E$  indicates that there is repulsion between the drugs, while its negative value indicates attraction between them.

### 3. Results and discussion

#### 3.1 Theoretical parameters

Firstly, we analyze the differences reactivity of all the species: cationic, neutral and anionic species of clopidogrel and clonidine drugs. We can define reactivity of the molecule as its activity or capacity to take part in a reaction or interaction with another specie. Table 1 shows the calculated quantum chemical parameters. HOMO energy ( $E_{\text{HOMO}}$ ) is associated with the electron-donating capacity, while LUMO energy ( $E_{\text{LUMO}}$ ) is associated with the ability to accept electrons. Then, the frontier orbitals are very important in defining an interaction between the molecules. The  $E_{\text{HOMO}}$  value (see Table 1) describes the sensitivity of the specie to any electrophilic attack in the region where the HOMO is located. Analyzing the three species of clonidine, we can observe that clonidine1 presents larger  $E_{\text{HOMO}}$  value (-7.483) compared to clonidine0 (-5.442) and clonidine-1 (-5.360). This result indicates that clonidine1 has greater sensitivity to an electrophilic attack than the other species. On the other hand, clopidogrel1 presents higher





$E_{\text{HOMO}}$  (-6.884), compared to the other species whose values are -6.014 eV (clopidogrel-0) and -5.442 eV (clopidogrel-1), respectively. Note in this case, that the energies are similar for all the species. A high value of  $E_{\text{HOMO}}$  represents the tendency of the molecule to donate electrons to an acceptor specie, which may be promising for the interaction between these donor and acceptor species.

The magnitude of the  $E_{\text{LUMO}}$  (see Table 1) indicates the ability of the molecule to accept electrons. If the molecule presents high  $E_{\text{LUMO}}$ , the probability of the specie accepting electrons decrease. In the case of clonidine drug, clonidine1 (-1.306) has a larger value than clonidine0 (-0.899) and clonidine-1 (-0.517); while for clopidogrel, bigger value is presented in clopidogrel1 (-1.524) compared to clopidogrel0 (-0.898) and clopidogrel-1 (-0.626), respectively. Therefore, clonidine1 has greater capacity to donate electrons than the other species, while clopidogrel1 has greater affinity to acquire electrons. It is important to note that, in all the cases, the species present the same  $E_{\text{HOMO}}/E_{\text{LUMO}}$  ratio, then, these parameters cannot indicate a marked trend by themselves. It is necessary to analyze other parameters.

A relatively higher band-gap ( $E_g$ ) value, clearly indicates that the molecule is more stable, that is, less reactive. In the case of clonidine (see Table 1), the most stable specie is clonidine1 (6.150) and the most reactive is clonidine0 (4.544). In the case of clopidogrel, the most stable is clopidogrel1 (5.360); nevertheless, for all the configurations, the  $E_g$  values are not significant different. Note that clopidogrel0 has a band-gap energy slightly higher than clonidine0, the type of interaction that will take part between the molecules is influenced by this parameter.

The chemical potential ( $\mu$ ) is related to the electronegativity. This parameter is associated with the changes on the electron density, that is, the possibility of electrons to flow from a region of high potential or low electronegativity to another region of low



potential or high electronegativity. In our study, clonidine1 (-4.381) and clopidogrel1 (4.218) are the most electro-attractive (see Table 1), being the species that present the lower chemical potential (greater electronegativity) compared with the other species. In the case of clonidine0 (-3.184), clonidine-1 (-2.939), clopidogrel0 (-3.456) and clopidogrel-1 (-3.048), these species have higher chemical potential and lower electronegativity.

Chemical hardness ( $\eta$ ) is a direct measure of the band gap; a large band gap implies a high chemical hardness value, that is, the specie is lesser reactive or liable, both, to receive electrons and to donate them. In our study, it is clearly observed that clonidine1 (3.075) has an  $\eta$  value significantly higher than the other species (see Table 1). This indicates that clonidine1 is lesser reactive than the other species, that is, it is more chemically stable. For comparison, the rest of the species have similar reactivity (clonidine0 (2.286), clonidine-1 (2.422), clopidogrel1 (2.667), clopidogrel0 (2.558) and clopidogrel-1 (2.422)). On the other hand, the chemical softness (S) parameter is the reciprocal of the hardness. As it is expected, the most chemically reactive is clopidogrel1 (3.320). Its S value is very close to clonidine1 (3.129). Then, all the other species have similar or close S values (see Table 1). Note that the clonidine-1 and clopidogrel-1 species have an S value slightly lower than the other species.

In the case of the electrophilicity index ( $\omega$ ), it is used to measure the decrease in the energy produced by the maximum flow of electrons between the HOMO (donor) and the LUMO (acceptor). High value of this parameter indicates that the molecule will be more resistant to change its electronic distribution. Clonidine1 presents the lowest  $\omega$  value (240.327) (see Table 1), while clonidine0 presents slightly larger  $\omega$  value (325.335), very similar to clonidine-1 (306.287) and clopidogrel-1 (307.239). The electrophilicity depends proportionally on the electronegativity and inversely to the chemical resistance



or stability. If the specie has high both electronegativity and chemical resistance, it would have low electrophilicity. If we analyze, for example, the case of clonidine1 which is the most electro-attractive, it presents the greatest both electronegativity and chemical resistance, and the lowest electrophilicity. The rest of the species have very similar electronegativity and lower electronegativity than clonidine1. They also present lower chemical resistance, with the exception of clopidogrel1 which has similar chemical stability to clonidine1. In general, when the chemical resistance is low, the specie is more reactive and presents high electrophilicity value. It is important to highlight the cases of clonidine1 (that presents high electronegativity and high chemical resistance) and clopidogrel1 (that presents low electronegativity and high chemical resistance), in both cases they have very different values of electrophilicity. We can conclude that the electronegativity is the parameter that determine the behavior of the specie. The electronegativity/chemical resistance ratio indicates which specie receive electrons (electrophilic capacity) or donate electrons (nucleophilic capacity). In our study, cationic clonidine has nucleophilic capacity ( $\omega=240.327$ ), while the anionic ( $\omega=306.287$ ) and neutral ( $\omega=325.335$ ) species present electrophilic capacity. In the case of clopidogrel, this drug has electrophilic capacity between 276.736 and 307.239.

### 3.2 Geometry optimization

The molecular electrostatic potential (MEP) for clopidogrel and clonidine molecules is shown in Fig. 1 (b). The negative charge density (red color) is concentrated in oxygen atoms of clopidogrel; while the positive charge density (blue color) is located on nitrogen atoms of clonidine. These charge concentrations predict a high probability of interaction between regions with opposite charge densities. Analyzing the complex structure of clonidine, this molecule presents an imidazole ring which contains two



characteristic nitrogens belonging to a ring of five atoms, an amino group, and a benzene ring containing two chlorine atoms in ortho positions. In the case of clopidogrel, among its most characteristic functional groups, it presents a carboxy-ester group, a benzene ring containing a chlorine atom, and a thiophene ring joined to an adjacent pyridine ring by ortho fusion. This structural complexity generates particular charge densities and concentration of active sites, positioning both molecules in their most favorable geometries for the interaction. In Fig. 2 and Fig. 3, it can be seen the optimized clopidogrel-clonidine configurations. As we can see, in Table 2, all the systems are stable because the obtained energies are negative. All the configurations present energies of small absolute values (see Table 2), typical of systems formed through interactions that are physical in nature. Typical binding energy of physisorption is about 10–600 meV, while chemisorption usually forms bonding with energy of 1–10 eV. In general, physisorption involves low-energy interactions [50]. The most favorable configuration is C2, which have the lowest energy of -0.527 eV (see Table 2). In Fig. 4 is shown the total electron density plot for C2 configuration. In C2 system, the opposite charge densities (Fig. 1) favorably interact without significant steric impediment, and thus, the interaction between the drugs is produced with the lowest energy. This fact occurs when both molecules are positioned exposing their most active zones, reaching the C2 geometry of lesser steric hindrance. The interaction between the drugs is produced by two O-H bonds and two N-H bonds, i.e., through four H-bonding formation (see Fig. 2). The oxygen of the carbonyl group of clopidogrel forms two hydrogen bonds with the hydrogens of clonidine at O-H distances of 1.87 Å and 2.21 Å, respectively; while the amino nitrogen of the imidazole ring of clonidine with carbonyl group (O=C) of clopidogrel forms two hydrogen bonds at N-H distances of 2.45 Å and 3 Å, respectively. Similar bonds and energies are reported in the literature [51]. These H-bonding interactions contribute to



determining the optimal geometry for C2 configuration being consistent with the obtained adsorption energy. Hydrogen-bonds play a crucial role in determining the specificity of molecule binding being important in stabilization. On the other hand, during administration, it is important hydrogen-bond impact on passive diffusion across cell membranes. Then, new hydrogen bonding will easy form with water's polar structure dissolving drug substances that organism needs, and that is necessary for the biochemical reactions. H-bonding interactions are ideal for controlled drug delivery application as it allows moderate and reversible drug adsorption, facilitating its release in the biological environment.

### 3.3 Infrared spectrometry (IR)

A widely used tool to schematize the internal structure of an organic molecule is the infrared (IR) spectrometry technique. IR spectrum is the finger print for any compound as it represents its different bonds, functional groups and their vibrations. IR spectrophotometry allows to identify shifts in the vibrational frequencies of the functional groups involved in covalent and non-covalent interactions [52, 53]. Chemical interactions result in breaking and formation of new bond, changing chemical nature of a compound. Any change in IR spectra of the compounds could predict changes in their chemical structure and indicate drug degradation or chemical bonding between the drugs. Therefore, IR spectrum is also performed to know the compatibility between the drugs.

By exposing the spectra to a detailed study, we have analyzed the presence of characteristic peaks associated to certain functional groups that are presented in the isolated molecules, as well as, bonds that could be formed after interaction (C2) [54]. Spectra in Fig. 5 show the presence of bands attributed to both drugs. The IR spectrum shows a band due to C=O stretching vibrations at  $1699\text{ cm}^{-1}$  corresponding to clopidogrel.



The band due to aromatic C–H stretching vibrations is represented at  $3160\text{ cm}^{-1}$ . The bands associated with C–O stretching appears at  $1068$ ,  $1153$  and  $1194\text{ cm}^{-1}$ . The IR spectrum includes picks at  $3005\text{ cm}^{-1}$  which can be attributed to the stretching vibrations of bonded N–H of clonidine. The bands with different intensities observed at  $1667\text{ cm}^{-1}$  and  $1245\text{ cm}^{-1}$  are assigned to the C–N stretching modes, while the band at  $445\text{ cm}^{-1}$  is assigned to the C–N–C deformation. The group of bands between  $3097$  and  $3105\text{ cm}^{-1}$  are assigned to the C–H stretching modes. The corresponding in-plane deformations modes are assigned to the IR bands at  $1438$ ,  $1199$  and  $1157\text{ cm}^{-1}$  while the bands at  $976$ ,  $900$  and  $768\text{ cm}^{-1}$  are assigned to the corresponding out-the plane deformations for all the species. The very weak band at  $266\text{ cm}^{-1}$  and  $222\text{ cm}^{-1}$  could be assigned to the stretching modes related to the C–H---Cl modes. The asymmetric and symmetric stretching modes of  $\text{CH}_2$  are assigned between  $3600$  and  $2944\text{ cm}^{-1}$ . The IR bands at  $1499$ ,  $1484$  and  $1457\text{ cm}^{-1}$  are assigned to the scissoring modes in agreement with compounds containing the  $\text{CH}_2$  group, while the medium IR bands at  $1342$  and  $1293\text{ cm}^{-1}$  are assigned to the wagging modes. The expected rocking modes are assigned to the weak IR band at  $1199\text{ cm}^{-1}$ . The twisting modes are associated with the weak band and a shoulder in IR at  $1026$  and  $805\text{ cm}^{-1}$  respectively. The C=C stretching modes of phenyl ring was assigned to the bands at  $1593$ ,  $1568$ ,  $1299$  and  $1073\text{ cm}^{-1}$ . The C–Cl stretching modes is assigned to the IR bands at  $411$  and  $398\text{ cm}^{-1}$ . However, the corresponding out-of-plane deformation modes appear at  $521$  and  $505\text{ cm}^{-1}$  in the IR. Two weak bands in the IR spectrum at  $1096$  and  $686\text{ cm}^{-1}$  are assigned to in-plane deformation modes of the phenyl ring (bendings). There are signals that appear in the IR spectrum at  $1123\text{ cm}^{-1}$  and  $1100\text{ cm}^{-1}$  that are assigned to in-plane deformation of the phenyl rings. For the imidazole ring, these bands appear at  $867$  and  $686\text{ cm}^{-1}$  in the IR. Moreover, the torsion rings modes for the phenyl ring are assigned to IR bands at  $695$  and  $480\text{ cm}^{-1}$ . In the case of vibrational modes around  $3131\text{ cm}^{-1}$  and

View Article Online  
DOI: 10.1039/D4NA00776J



close to  $3505\text{ cm}^{-1}$ , the peaks correspond to the vibrations of the O-H and the H-N bonds, respectively. [55]. In the case of clonidine-clopidogrel system (C2), the peaks appear with a very significant intensity in relation to the isolated molecule peaks, and, specially, the peak at  $3360\text{ cm}^{-1}$  that could be associated with the formed H-bonds. H-bonds are formed by the approach of the molecules producing the characteristic vibrational mode of these functional groups, as can be seen in the IR spectrum (Fig. 5). This finding corroborates the O-H and N-H bonds formed during C2 interaction. On the other hand, the appearance of the same characteristic peaks of isolated clonidine and clopidogrel in the C2 spectrum, without any changes in their position, indicates the absence of drugs degradation or chemical bonds between the drugs.

### 3.4 Total density of states (TDOS)

The total densities of states (TDOS) of each isolated molecule and C2 configuration are presented in Fig. 6. Superposition can be seen between the molecule bands. It can be observed that clopidogrel molecule has larger band-gap than clonidine, corroborating the  $E_g$  value presented in Table 1. The clopidogrel-clonidine system (C2) is more stable than the isolated molecules because their molecular states are stabilized to lower energy values after the interaction. At the time of the interaction between the molecules, new states are generated in the area close to the Fermi level. However, the size of the remanent gap plus the absence of states precisely at the Fermi level is coincident with the previous finding, that is, the interaction between the drugs is produced by physical adsorption.

### 3.5 Atomic charge distribution



In order to analyze the interaction in detail, we have calculated the atomic charge distributions (Natural bonding orbital - NBO) [56] for C2 configuration and the isolated drugs (Table 3). As we can see, the charge exchanges are small. It can be associated with the physical-type adsorption between the drugs. The atom that is most affected in clopidogrel is O4 which has charge variation of -0.041, belonging to the carbonyl group that participates in two H-bond formation, previously described. This is due to the proximity of H56 and H57 of clonidine that promotes a redistribution of charges, electro-negativizing the oxygen. On the other hand, the main redistribution on clonidine occurs on N40 and N41 that present charge modification of -0.015 and -0.018, respectively. This is in agreement with the formation of two N-H bonds in C2, previously described. It is important to mention that an organic molecule undergoes charge redistributions to stabilize itself in the new electrochemical environment generated by the approach of another organic molecule. This is much more accentuated in the regions close to the zone of interaction. Distant to this zone, the molecules present an electronic rearrangement that allows them to be stabilized without generating major changes.

In Table 4, it is presented the occupancy percentages of the bonds more affected after clopidogrel-clonidine interaction. The presence of sigma and pi bonds between O4 and C14 of clopidogrel, can be observed. The highest variation in the occupancy percentage, when the molecules interact, occurs in the  $\pi$  bond of O4. For isolated clopidogrel, there are 65.82% of occupancy in O4 p orbital and 34.18% in the C14 p orbital. When the molecules interact, the occupancy percentage of O4 increases to 67.52%, while C14 decreases to 32.48%; although its occupancies are redistributed by 0.24% and 0.26%, respectively, on the s orbital. This may be due to the fact that the proximity of H56 and H57 of clonidine distorts the double bond increasing its occupancy. In turn, the H56 and H57 atoms (Table 4) decrease its occupancy percentage in the





original bond after the H-bonds establishment. Similar findings are found for H36 and H37 atoms that reduce their percent participation in the original C-H bond after the H-bonds formation (Table 4).

Interaction of electron delocalization can be reflected quantitatively using stabilizing energy ( $E^{(2)}$ ) which is estimated based on the theory of the Second Order Perturbation [57]. In NBO-analysis on hydrogen bond systems, the most significant thing is the charge transfer between lone pairs (LP(Y)) from a Y-atom and anti-bonding orbitals (BD\* (X-H)) of X-H bonds, that is correlated with X-H...Y interaction intensity and may give qualitative description of its contribution to the total energy. The charge transfer between the lone pair of an acceptor to the anti-bonding orbital of the donor provides the substantial to the stabilization of the hydrogen bonds. Accordingly, the stabilizing energy ( $E^{(2)}$ ) is calculated to characterize the hydrogen bond interaction (see Table 5). The existence of electron lone-pairs donation shows the existence of hydrogen bonds between clopidogrel and clonidine molecules. In general, the strength of the hydrogen bond depends on the electronegativity of the atoms. It can classify as very strong (e.g., [F...H...F]<sup>-</sup>), strong (e.g., O-H...O=C), or weak (e.g., C-H...O) depending on the bond energy, which ranges from 1.7 eV to <0.1 eV, respectively [50]. In Table 5, it can be seen the H-bonding energies that are in accordance to the total energy of C2 system (see Table 2). The interaction LP (1) O4 → BD\*(1) N41 - H57 is found as the strongest one with a stabilizing energy of 0.47 eV. From these observations, it can be deduced that the hydrogen bond formed between O4 of clopidogrel and H57 of clonidine is the strongest interaction between the both molecules which agrees with the smallest distance obtained for the H57 - O4 bonding (see Table 5).



The Electron Localization Function (ELF) map, made by Multiwfn program [58], provides a color-coded representation of electron distribution of clopidogrel-clonidine system (Fig. 7). High ELF values, typically shown in warm colors such as red or orange, indicate regions with strongly localized electrons, such as covalent bonds or lone pairs; while low ELF values, often represented in cooler colors like blue, reflect delocalized or non-covalent forces. This visualization aids in understanding bonding characteristics and electronic interactions. The molecular interaction between clonidine and clopidogrel, focus particularly on the H57 (clonidine) and O4 (clopidogrel) atoms, where this interaction involves non-covalent forces such as hydrogen bonds, according previous analysis. In the ELF visualization, dark blue regions between atoms highlight voids with low electron localization, suggesting regions dominated by electron delocalization reinforcing the argument for a weak interaction between clonidine and clopidogrel.

#### 4. Conclusions

Since clopidogrel and clonidine medications are typically taken in combination, it is crucial to examine their molecular interactions. Theoretical parameters serve as to interpret the drug properties and predict the bonding, in their chemical environment. In general, the frontiers orbital energies indicate that clonidine have greater sensitivity to electrophilic attack, while clopidogrel presents more tendency to donate electrons. The band-gap energy indicates that neutral clonidine molecule is little more reactive than clopidogrel. This result predicts a physics type interaction between the molecules. NBO analysis corroborates this finding. In general, the chemical potential is similar for all the species. This parameter indicate that the electron density can exchange, but the direction is not remarkable and easy to predict. The chemical hardness and softness parameters are also very similar for both molecules. Therefore, clopidogrel and clonidine drugs have



similar reactivity in water. Clonidine present higher electrophilicity values than clopidogrel, indicative that it is the more resistant to change its electronic distribution.

MEP map shows that negative charge density is concentrated in the oxygens (clopidogrel), while the positive charge density is located in the nitrogens (clonidine). The TDOS plot shows that clopidogrel-clonidine system is more stable than the isolated molecules. New states appear in the zone close to the Fermi level after interaction, however, the size of the remanent gap plus the absence of states exactly at the Fermi level is coincident with the physical-type interactions between the drugs. The lowest energy interaction is reached by the formation of four H-bonds (1.87 Å – 3.00 Å). The intensive peak at 3360 cm<sup>-1</sup> in IR spectrum could be associated to the formed H-bonds. Spectra also confirms the absence of degradation or chemical bonds between the drugs.

### Acknowledgments

Our work was financed by Universidad Tecnológica Nacional, Argentina and Agencia I+D+i, Argentina. S. S. is member of CONICET. B. O. C. is fellow of Agencia I+D+I - UTN. G. D., E. N. G. and G. R. are fellows of CONICET.

There are no conflicts of interest to declare.

### References

- [1] M. Di Cesare, P. Perel, S. Taylor, C. Kabudula, H. Bixby, T.A. Gaziano, D.V. McGhie, J. Mwangi, B. Pervan, J. Narula, D.Pineiro, F.J. Pinto. The Heart of the World. *Global Heart*. 19(1) (2024) 11.
- [2] S. D'Sa, SJ Machin. Clopidogrel, a novel antiplatelet agent. *Hosp Med* 60(5) (1990) 362-363.



- [3] H.D. White, J.K. French, C.J. Ellis. New antiplatelet agents. *Aust NZ J Med* 28(4) (1998) 558-564. View Article Online  
DOI: 10.1059/D4NA00776J
- [4] K. Schör. Clinical pharmacology of the adenosin diphosphate (ADP) receptor antagonist, clopidogrel. *Vasc Med* 3(3) (1998) 247-251.
- [5] A.J. Coukell, A. Markaham. Clopidogrel. *Drugs* 54(5) (1997) 745-750.
- [6] J.M. Herbert, D. Frehel, E. Valle et al. Clopidogrel, a novel antiplatelet and antithrombotic agent. *Cardiovasc Drug Rev* 11(2) (1993) 180-198.
- [7] C. Gadget, A. Stierle, Cazenave JP, et al. The Tienopyridine PCR 4099 selectively inhibits ADP-induced platelet aggregation and fibrinogen binding without modifying the membrane glycoprotein IIb-IIIa complex in rat and in man. *Biochem Pharmacol* 40(15) (1990) 229-238.
- [8] P. Savi, J.M. Herbert, A.M. Pflieger, et al. Importance of hepatic metabolism in the aggregating activity of the Thienopyridine clopidogrel. *Biochem Pharmacol* 44 (1992) 527-532.
- [9] <https://clincalc.com/DrugStats/Top200Drugs.aspx>
- [10] E. F. Krake, H. Jiao, W. Baumann, NMR and DFT analysis of the major diastereomeric degradation product of clopidogrel under oxidative stress conditions, *J. Mol. Struct.* 1247 (2022) 131309.
- [11] E. F. Krake, L. Backer, B. Andres, W. Baumann, N. Handler, H. Buschmann, U. Holzgrabe, C. Bolm, T. Beweries, Mechanochemical Oxidative Degradation of Thienopyridine Containing Drugs: Toward a Simple Tool for the Prediction of Drug Stability, *ACS Cent. Sci.* 9 (2023) 1150–1159.
- [12] L. Cárdenas, A. Aymen Abdullah, G. Jaramillo, P. Cárdenas, G. Gálvez, F. Hidalgo, Clopidogrel resistance in extremely high cardiovascular risk patients with genotype CYP2C19, *Rev. Fed. Arg. Cardiol.* 52(3) (2023) 134-137.



- [13] A. Kundalevich, A. Kapitonova, K. Berezin, A. Zyubin, E. Moiseeva, V. Rafalskiy, I. Samusev, Raman spectra simulation of antiplatelet drug-platelet interaction using DFT, *Sci. Rep.* 14 (2024) 1445. New Article Online  
DOI: 10.1039/D4NA00776J
- [14] M.P.B. Simonetti, E.A. Valinetti, F.M.C. Ferreira. Clonidine: from nasal descongester to potent analgesic. Historical and pharmacological considerations. *Rev Bras Anesthesiol*, 47 (1997) 37-47.
- [15] T.C.A. Alves, J.R.C. Braz, P.T.G. Vianna.  $\alpha_2$ -agonistas em anestesiologia: aspectos clínicos e farmacológicos. *Rev Bras Anesthesiol*, 50 (2000) 396-404.
- [16] T. Kubo, Y. Misu. Pharmacological characterisation of the  $\alpha$ -adrenoceptors responsible for a decrease of blood pressure in the nucleus tractus solitarii of the rat. *Naunyn Schmiedeberg Arch Pharmacol*, 317 (1981) 120-125.
- [17] R.R. Ruffolo Jr. Distribution and function of peripheral  $\alpha$ -adrenoceptors in the cardiovascular system. *Pharmacol Biochem Behav*, 22 (1985) 827-833.
- [18] R. Xiao, L. He, Z. Luo, R. Spinney, Z. Wei, D.D. Dionysiou, F. Zhao, An experimental and theoretical study on the degradation of clonidine by hydroxyl and sulfate radicals, *Science of The Total Environment* 710 (2020) 136333.
- [19] E. Romano, L. Davies, S. A. Brandan, Structural properties and FTIR-Raman spectra of the anti-hypertensive clonidine hydrochloride agent and their dimeric species, *Journal of Molecular Structure* 1133 (2017) 226e235.
- [20] P. Calzavacca, L. C. Booth, Y. R Lankadeva, S. R. Bailey, L. M. Burrell, M. Bailey, R. Bellomo, C. N. May, Effects of clonidine on the cardiovascular, renal, and inflammatory responses to experimental bacteremia, *Shock* 51(3) (2019) 348-355.
- [21] A. Joseph, A. S Binu, J. Kuppusamy, N. Pushpanathan, N. Pushpanathan, Combined effect of clonidine and bupivacaine during hernioplasty -a case study, *International Journal of Scientific Research* 11 (2022) 2277 – 8179.



- [22] Krzywanski, J.; Sosnowski, M.; Grabowska, K.; Zylka, A.; Lasek, L.; Kijko, View Article Online  
DOI: 10.1039/D4NA00776J Kleczkowska, A. Advanced Computational Methods for Modeling, Prediction and Optimization—A Review. *Materials* 17 (2024) 3521.
- [23] A. Abbasi, J. Jahanbin Sardroodi, Adsorption of O<sub>3</sub>, SO<sub>2</sub> and SO<sub>3</sub> gas molecules on MoS<sub>2</sub> monolayers: A computational investigation, *Applied Surface Science* 469 (2019) 781-791.
- [24] A. Abbasi and J. Jahanbin Sardroodi, An innovative gas sensor system designed from a sensitive nanostructured ZnO for selective detection of Sox molecules: A density functional theory study *New J. Chem.*, 2017, DOI: 10.1039/C7NJ02140B
- [25] A. Abbasi, A. Abdelrasoul, J. Jahanbin Sardroodi, Adsorption of CO and NO molecules on Al, P and Si embedded MoS<sub>2</sub> nanosheets investigated by DFT calculations, *Adsorption* 25 (2019) 1001–1017.
- [26] A. Abbasi, J. Jahanbin Sardroodi, A highly sensitive chemical gas detecting device based on N-doped ZnO as a modified nanostructure media: A DFTCNBO analysis, *Surface Science* (2017), doi: 10.1016/j.susc.2017.10.029
- [27] A. Abbasi, J. Jahanbin Sardroodi, An Innovative Method for the Removal of Toxic Sox Molecules from Environment by TiO<sub>2</sub>/ Stanene Nanocomposites: A First-Principles Study, *Journal of Inorganic and Organometallic Polymers and Materials* (2018) <https://doi.org/10.1007/s10904-018-0832-9>
- [28] A. Abbasi, J. Jahanbin Sardroodi, Exploration of sensing of nitrogen dioxide and ozone molecules using novel TiO<sub>2</sub>/Stanene heterostructures employing DFT calculations, *Applied Surface Science* (2018), doi: <https://doi.org/10.1016/j.apsusc.2018.02.183>
- [29] A. Abbasi, Tuning the structural and electronic properties and chemical activities of stanene monolayers by embedding 4d Pd: a DFT study, *RSC Adv.* 9 (2019) 16069–16082.



- [30] A. Abbasi, Adsorption of phenol, hydrazine and thiophene on stanene monolayers, *Synthetic Metals* 247 (2019) 26–36. View Article Online  
DOI: 10.1039/D4NA00776J
- [31] A. Abbasi, J. Jahanbin Sardroodi, Density functional theory investigation of the interactions between the buckled stanene nanosheet and  $XO_2$  gases ( $X=N, S, C$ ), *Computational & Theoretical Chemistry* (2017), doi: <https://doi.org/10.1016/j.comptc.2017.12.010>
- [32] A. Abbasi, J.J. Sardroodi, The adsorption of sulfur trioxide and ozone molecules on stanene nanosheets investigated by DFT: Applications to gas sensor devices, *Physica E: Low-dimensional Systems and Nanostructures* (2018), doi: 10.1016/j.physe.2018.05.004.
- [33] A. Abbasi, Modulation of the electronic properties of pristine and AlP-codoped stanene monolayers by the adsorption of  $CH_2O$  and  $CH_4$  molecules: A DFT study *Mater. Res. Express* 6 (2019) 076410 <https://doi.org/10.1088/2053-1591/ab1199>
- [34] J. M. Castellano, S. J. Pocock, D. L. Bhatt, A. J. Quesada, R. Owen, A. Fernandez-Ortiz, P. L. Sanchez, Polypill Strategy in Secondary Cardiovascular Prevention, *N. Engl. J. Med.* 387 (2022) 967-977.
- [35] R.D Dennington, T.A Keith, J.M. Millam, (2008) GaussView 5.0.8, Gaussian.
- [36] M. J. Frisch, G. W. Trucks, H. B. Schlegel, G. E. Scuseria, M. A. Robb, J. R. Cheeseman, G. Scalmani, V. Barone, B. Mennucci, G. A. Petersson, H. Nakatsuji, M. Caricato, X. Li, H. P. Hratchian, A. F. Izmaylov, J. Bloino, G. Zheng, J. L. Sonnenberg, M. Hada, M. Ehara, K. Toyota, R. Fukuda, J. Hasegawa, M. Ishida, T. Nakajima, Y. Honda, O. Kitao, H. Nakai, T. Vreven, J. A. Montgomery, Jr., J. E. Peralta, F. Ogliaro, M. Bearpark, J. J. Heyd, E. Brothers, K. N. Kudin, V. N. Staroverov, R. Kobayashi, J. Normand, K. Raghavachari, A. Rendell, J. C. Burant, S. S. Iyengar, J. Tomasi, M. Cossi, N. Rega, J. M. Millam, M. Klene, J. E. Knox, J. B. Cross, V. Bakken, C. Adamo, J. Jaramillo, R. Gomperts, R. E. Stratmann, O. Yazyev, A. J. Austin, R. Cammi, C. Pomelli,



- J. W. Ochterski, R. L. Martin, K. Morokuma, V. G. Zakrzewski, G. A. Voth, P. Salvador, J. J. Dannenberg, S. Dapprich, A. D. Daniels, Ö. Farkas, J. B. Foresman, J. V. Ortiz, J. Cioslowski, and D. J. Fox, *Gaussian 09*, Gaussian, Inc., Wallingford CT, (2009). R.D.
- [37] A. D. Becke, *J. Chem. Phys.* 96 (1992) 2155–2160.
- [38] C. Lee, W. Yang and R. G. Parr, *Phys. Rev. B: Condens. Matter Mater. Phys.* 37 (1988) 785.
- [39] W. J. Hehre, R. Ditchfield, and J. A. Pople, Self-Consistent Molecular Orbital Methods. XII. Further extensions of Gaussian-type basis sets for use in molecular-orbital studies of organic-molecules, *J. Chem. Phys.* 56 (1972) 2257.
- [40] S. Grimme, S. Ehrlich, L. Goerigk, Effect of the damping function in dispersion corrected density functional theory, *J. Comput. Chem.* 32 (2011) 1456.
- [41] M. Salah, A. S. Zeroual, H. Jorio, El hadki, OK Kabbaj, K Marakchi et al. Theoretical study of the 1,3-DC reaction between fluorinated alkynes and azides: reactivity indices, transition structures, IGM and ELF analysis. *J Mol Graph Model* 94 (2020) 107458.
- [42] H. Mohammad-Salim, R. Hassan, H.H. Abdallah, M. Oftadeh. The theoretical study on the mechanism of [3+2] cycloaddition reactions between  $\alpha$ ,  $\beta$ -unsaturated selenoaldehyde with nitrene and with nitrile oxide. *J Mex Chem Soc* 64 (2020) 2594-0317.
- [43] G. Dodero, E. Nosedà Grau, G. Román, A. Díaz Compañy, S. Simonetti, Computational insights into co-adsorbed captopril and aspirin drugs on Si-doped (10,0) SWCNT as polypill model for cardiovascular disease, *Diam. Relat. Mater.* 124 (2022) 108945–108953.





- [44] M. Cossi, V. Barone, R. Cammi, and J. Tomasi, “Ab initio study of solvated molecules: A new implementation of the polarizable continuum model,” *Chem. Phys. Lett.* 255 (1996) 327-35.
- [45] B. Mennucci, JM Martínez, J. Tomasi, Solvent effects on nuclear shieldings: Continuum or discrete solvation models to treat hydrogen bond and polarity effects?, *Phys. Chem. A* 105 (2001) 7287-7296.
- [46] B. Mennucci, J. Tomasi, R. Cammi, J. R. Cheeseman, M. J. Frisch, F. J. Devlin, S. Gabriel, P.J. Stephens, Polarizable continuum model (PCM) calculations of solvent effects on optical rotations of chiral molecules, *J. Phys. Chem. A* 106 (2002) 6102-6113.
- [47] A.U. Orozco Valencia. Transferencia de carga y reactividad química en la teoría de funcionales de la densidad. (2017).
- [48] G. Restrepo; R. Harré. *Int. J. Phil. Chem.* No. 1 (2015) 19-38.
- [49] N. Dastani, A. Arab, H. Raissi, Adsorption of Ampyra anticancer drug on the graphene and functionalized graphene as template materials with high efficient carrier. *Adsorption* 26 (2020) 879–893.
- [50] J.M. MacLeod, F. Rosei, *Nanostructured Surfaces in Comprehensive Nanoscience and Technology*, 2011.
- [51] A. Gavezzotti, Comparing the strength of covalent bonds, intermolecular hydrogen bonds and other intermolecular interactions for organic molecules: X-ray diffraction data and quantum chemical calculations. *New Journal of Chemistry*, 40(8) (2016) 6848–6853.
- [52] H. R. H.; Ali, A. Alhalaweh, N. F. C Mendes,.; P Ribeiro-Claro,.; S. P. Velaga, Solid-state vibrational spectroscopic investigation of cocrystals and salt of indomethacin. *CrystEngComm*.14 (2012) 6665-6674.

View Article Online  
DOI: 10.1039/D4NA00776J



- [53] R. A. E. Castro, J. D. B.; Ribeiro, T. M. R. Maria, M. R. Silva, C. Yuste-Vivas, J. Canotilho, M. E. S. Eusebio, Naproxen Cocrystals with Pyridinecarboxamide Isomers. *Cryst. Growth Des.* 11, (2011) 5396-5404. View Article Online  
DOI: 10.1039/D4NA00776J
- [54] Y. C. Chien, M. Lu, M. Chai y F.J. Boreo Characterization of biodiesel and biodiesel particulate matter by TG, TG-MS, and FTIR, *Energy & Fuels*, 23 (2009) 202–206.
- [55] R. M. Silverstein, G. C. Bassler y T. C. Morrill. Spectrometric identification of organic compounds, 5th ed. New York: John Wiley, (1991).
- [56] F. Weinhold, CR Landis, y ED Glendening, What is NBO analysis and how is it useful? *International Reviews in Physical Chemistry*, 35(3) (2016) 399–440.
- [57] N. Singla, P. Chowdhury, Density functional investigation of photo induced Intramolecular Proton Transfer (IPT) in Indole-7- carboxaldehyde and its experimental verification, *J. Mol. Struct.*, 1045 (2013) 72–80.
- [58] T. Lu, F. Chen, Multiwfn: A multifunctional wavefunction analyzer, *J. Comput. Chem.* 33 (2012) 580–592.



Table 1. The values of the highest occupied molecular orbital energies ( $E_{\text{HOMO}}$ ) and the lowest unoccupied molecular orbital energies ( $E_{\text{LUMO}}$ ), energy gap ( $E_g$ ), global hardness ( $\eta$ ), chemical potential ( $\mu$ ), electrophilicity ( $\omega$ ) index and softness ( $S$ ) (all in eV).

Specie <sup>1</sup>	$E_{\text{HOMO}}$	$E_{\text{LUMO}}$	$E_g$ <sup>2</sup>	$\eta$ <sup>3</sup>	$\mu$ <sup>4</sup>	$\omega$ <sup>5</sup>	$S$ <sup>6</sup>
clonidine1	-7.483	-1.306	6.150	3.075	-4.381	240.327	3.129
clonidine0	-5.442	-0.898	4.544	2.286	-3.184	325.335	2.231
clonidine-1	-5.360	-0.517	4.843	2.422	-2.939	306.287	1.796
clopidogrel1	-6.884	-1.524	5.360	2.667	-4.218	276.736	3.320
clopidogrel0	-6.014	-0.898	5.116	2.558	-3.456	289.960	2.340
clopidogrel-1	-5.442	-0.626	4.816	2.422	-3.048	307.239	1.905

<sup>1</sup>Clonidine/Clopidogrel 1 = cationic specie, (+1) charged, Clonidine/Clopidogrel 0 = neutral specie and Clonidine/Clopidogrel -1 = anionic specie, (-1) charged.

<sup>2</sup>Eq. (1).

<sup>3</sup>Eq. (2).

<sup>4</sup>Eq. (4).

<sup>5</sup>Eq. (5).

<sup>6</sup>Eq. (3).



Table 2. Energies for clopidogrel-clonidine configurations

View Article Online  
DOI: 10.1039/D4NA00776J

Configurations <sup>1</sup>	$\Delta E$ (eV) <sup>2</sup>
C1	-0.187
C2	-0.527
C3	-0.161
C4	-0.309
C5	-0.142
C6	-0.134
C7	-0.068
C8	-0.125
E <sub>clopidogrel</sub> = -231.039 eV E <sub>clonidine</sub> = -143.176 eV	

<sup>1</sup> Fig. 2 and Fig. 3.<sup>2</sup> Eq. (6).

Table 3. NBO Charge for isolated clopidogrel, isolated clonidine and clopidogrel-clonidine interaction (C2). View Article Online  
DOI: 10.1039/D4NA00776J

Atom*	Nº	Clopidogrel-clonidine	Clopidogrel	Clonidine	$\Delta$ charge
Cl	1	-0.053	-0.057	-	0.004
S	2	0.330	0.328	-	0.002
O	3	-0.472	-0.491	-	0.019
O	4	<b>-0.571</b>	<b>-0.530</b>	-	<b>-0.041</b>
N	5	-0.498	-0.497	-	-0.001
C	6	-0.266	-0.266	-	-
C	7	-0.277	-0.277	-	-
C	8	-0.157	-0.160	-	0.003
C	9	-0.496	-0.496	-	-
C	10	-0.104	-0.104	-	-
C	11	-0.172	-0.172	-	-
C	12	-0.078	-0.076	-	-0.002
C	13	-0.277	-0.277	-	-
C	14	<b>0.776</b>	<b>0.739</b>	-	<b>0.037</b>
C	15	-0.400	-0.401	-	0.001
C	16	-0.018	-0.018	-	-
C	17	-0.207	-0.207	-	-
C	18	-0.252	-0.253	-	0.001
C	19	-0.240	-0.242	-	0.002
C	20	-0.226	-0.228	-	0.002
C	21	-0.371	-0.367	-	-0.004
H	22	0.251	0.251	-	-
H	23	0.223	0.220	-	0.003
H	24	0.233	0.231	-	0.002
H	25	0.262	0.261	-	0.001
H	26	0.267	0.262	-	0.005
H	27	0.264	0.263	-	0.001
H	28	0.266	0.265	-	0.001
H	29	0.265	0.265	-	-
H	30	0.272	0.271	-	0.001
H	31	0.272	0.271	-	0.001
H	32	0.274	0.273	-	0.001
H	33	0.261	0.260	-	0.001
H	34	0.264	0.263	-	0.001
H	35	0.242	0.239	-	0.003
H	36	0.234	0.228	-	0.006
H	37	0.231	0.229	-	0.002
Cl	38	-0.036	-	-0.024	-0.012
Cl	39	-0.025	-	-0.036	0.011
N	40	<b>-0.697</b>	-	<b>-0.682</b>	<b>-0.015</b>
N	41	<b>-0.670</b>	-	<b>-0.652</b>	<b>-0.018</b>
N	42	-0.576	-	-0.567	-0.009



C	43	-0.287	-	-0.286	-0.001
C	44	-0.314	-	-0.316	0.002
C	45	0.591	-	0.589	0.002
C	46	0.143	-	0.143	-
C	47	-0.044	-	-0.041	-0.003
C	48	-0.038	-	-0.048	0.010
C	49	-0.249	-	-0.247	-0.002
C	50	-0.249	-	-0.246	-0.003
C	51	-0.232	-	-0.234	0.002
H	52	0.245	-	0.240	0.005
H	53	0.232	-	0.238	-0.006
H	54	0.241	-	0.239	0.002
H	55	0.234	-	0.239	-0.005
H	56	0.416	-	0.421	-0.005
H	57	0.442	-	0.441	0.001
H	58	0.278	-	0.278	-
H	59	0.277	-	0.279	-0.002
H	60	0.270	-	0.271	-0.001

\*Reference for atoms is showed in Fig. 4.

View Article Online  
DOI: 10.1039/D4NA00776J



Table 4. Occupancy percentage of the bonds that participate in the interactions.

View Article Online  
DOI: 10.1039/D4NA00776J

clonidogrel	Before interaction	After interaction
O4=C14	BD (1) O 4 - C 14 ( 66.24%) O 4 s( 40.80%) p ( 59.20%) ( 33.76%) C 14 s( 33.21%) p ( 66.79%)	BD (1) O 4 - C 14 ( 66.66%) O 4 s( 40.85%) p ( 59.15%) ( 33.34%) C 14 s( 32.69%) p ( 67.31%)
	BD (2) O 4 - C 14 ( 65.82%) O 4 s( 0.00%) p (100.00%) ( 34.18%) C 14 s( 0.00%) p (100.00%)	BD (2) O 4 - C 14 ( 67.52%) O 4 s( 0.24%) p ( 99.76%) ( 32.48%) C 14 s( 0.26%) p ( 99.74%)
C21-H36	BD (1) C 21 - H 36 ( 61.75%) C 21 s( 27.16%) p ( 72.84%) ( 38.25%) H 36 s( 100.00%)	BD (1) C 21 - H 36 ( 61.81%) C 21 s( 27.16%) p ( 72.84%) ( 38.19%) H 36 s( 100.00%)
C21-H37	BD (1) C 21 - H 37 ( 61.73%) C 21 s( 27.26%) p ( 72.74%) ( 38.27%) H 37 s( 100.00%)	BD (1) C 21 - H 37 ( 61.88%) C 21 s( 27.27%) p ( 72.73%) ( 38.12%) H 37 s( 100.00%)

clonidine	Before interaction	After interaction
N40-H56	BD (1) N 40 - H 56 ( 71.71%) N 40 s( 30.54%) p ( 69.46%) ( 28.29%) H 56 s( 100.00%)	BD (1) N 40 - H 56 ( 72.87%) N 40 s( 32.46%) p ( 67.54%) ( 27.13%) H 56 s( 100.00%)
N41-H57	BD (1) N 41 - H 57 ( 72.11%) N 41 s( 26.46%) p ( 73.54%) ( 27.89%) H 57 s( 100.00%)	BD (1) N 41 - H 57 ( 72.13%) N 41 s( 26.52%) p ( 73.48%) ( 27.87%) H 57 s( 100.00%)



Table 5. Second-order perturbation stabilization energies of the H-bonds

View Article Online  
DOI: 10.1039/D4NA00776J

<b>Donor NBO (i)</b>	<b>Acceptor NBO (j)</b>	<b>E(2) (eV)</b>	<b>Bond</b>	<b>Distance (Å)</b>
LP (1) O4	BD*(1) N40 - H56	0.07	H56 - O4	2.21
LP (1) O4	BD*(1) N41 - H57	0.47	H57 - O4	1.87
LP (1) N40	BD*(1) C21 - H36	0.12	H36 - N40	2.45
LP (1) N41	BD*(1) C21 - H37	0.01	H37 - N41	3.00





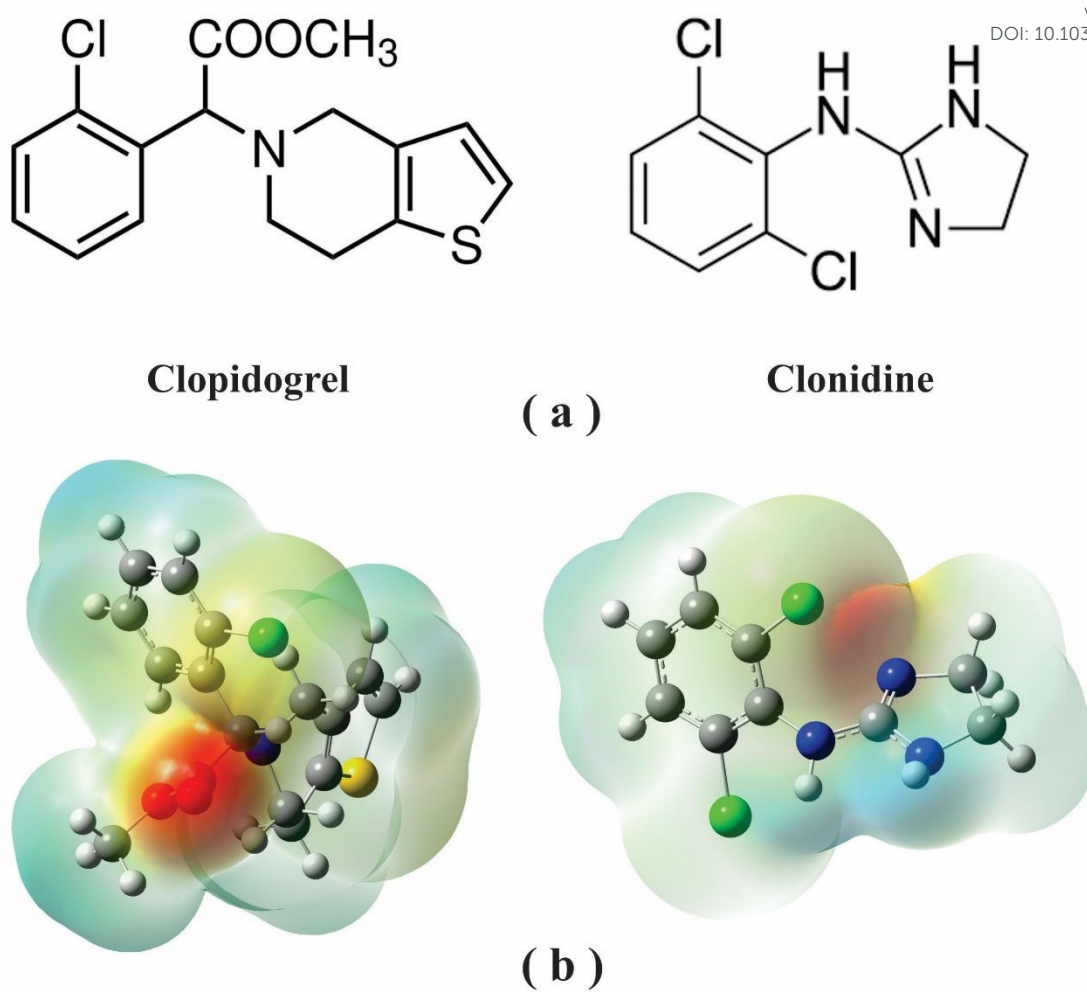


Fig. 1. (a) Chemical structure and (b) molecular electrostatic potential (MEP) of clopidogrel and clonidine drugs.



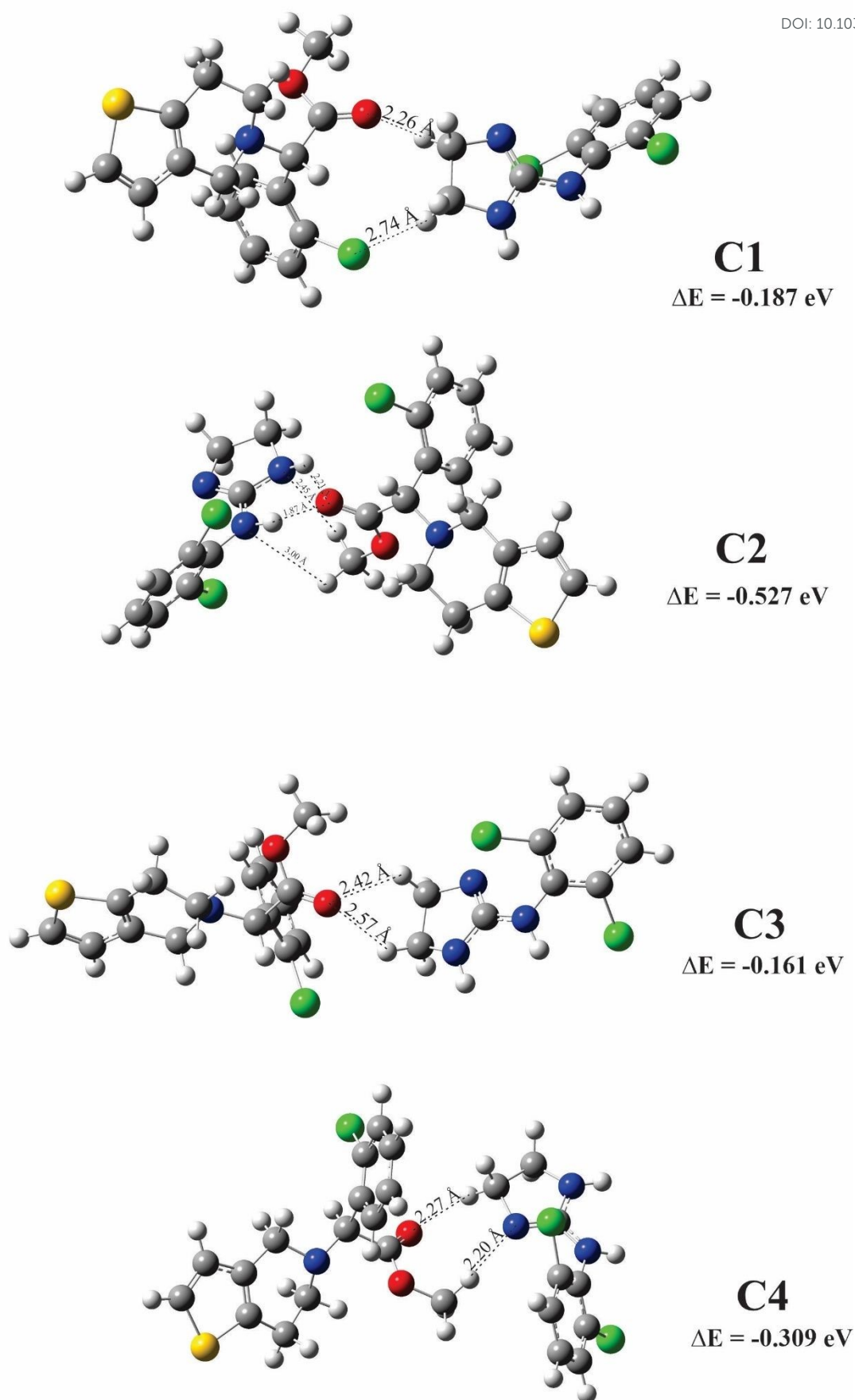
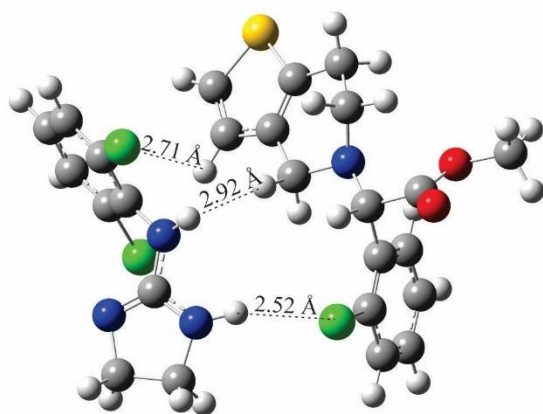
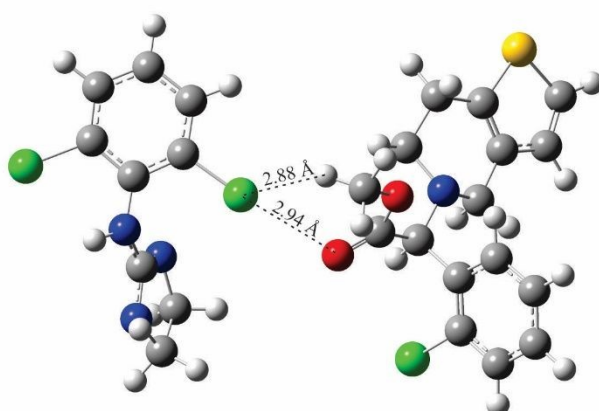


Fig. 2. Configurations of minimum energy for clopidogrel-clonidine interaction.

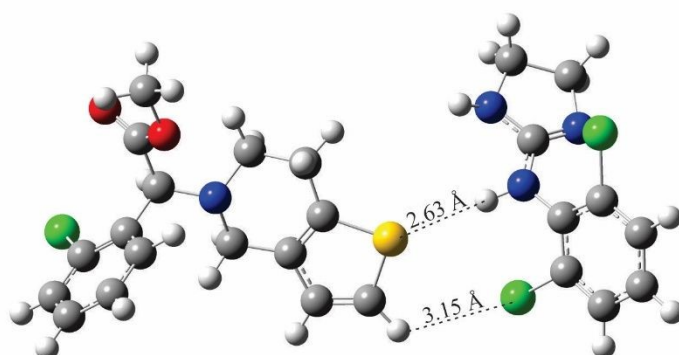




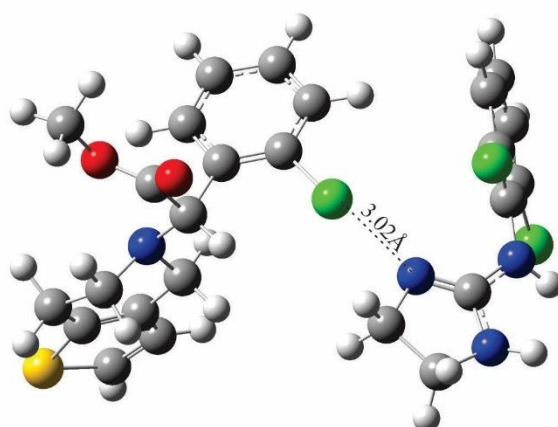
**C5**  
 $\Delta E = -0.142$  eV



**C6**  
 $\Delta E = -0.134$  eV



**C7**  
 $\Delta E = -0.068$  eV



**C8**  
 $\Delta E = -0.125$  eV

Fig. 3. Configurations of minimum energy for clopidogrel-clonidine interaction.



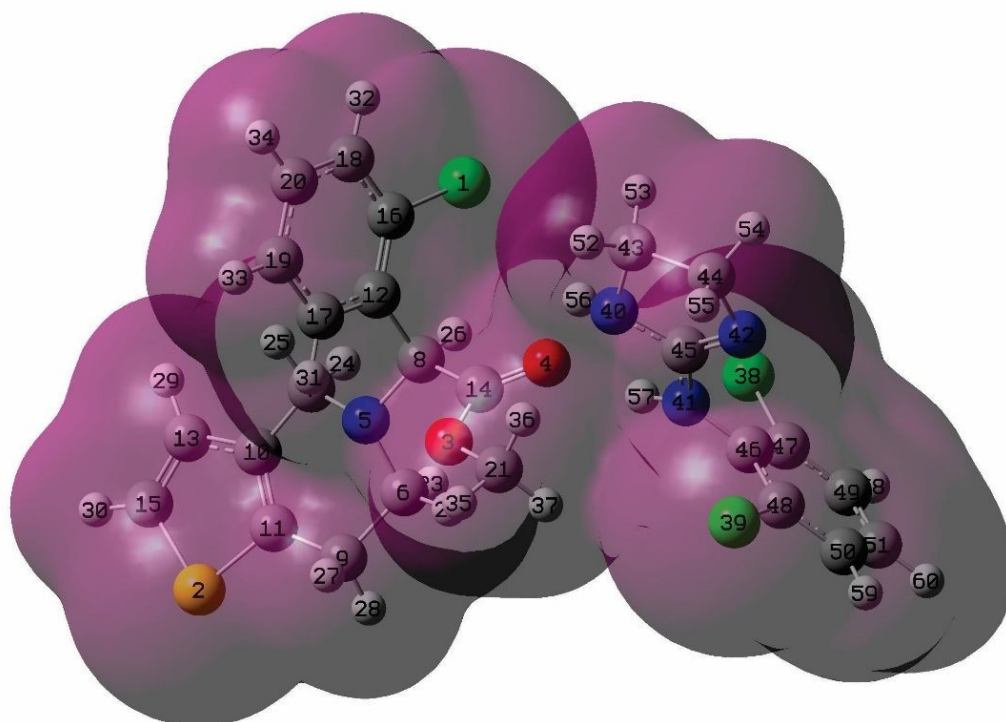
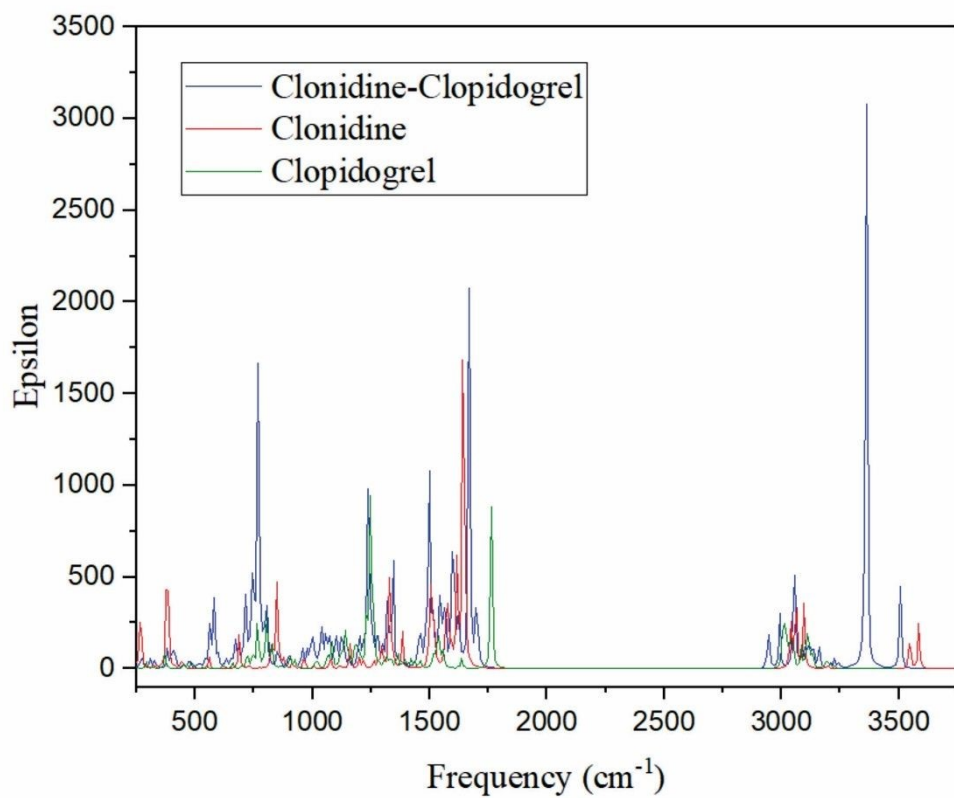


Fig. 4. Electron density from total SCF density for C2 configuration. Numering for atoms is showed.





View Article Online  
DOI: 10.1039/D4NA00776J

Fig. 5 IR Spectra of isolated clopidogrel, isolated clonidine and clopidogrel-clonidine interaction (C2).



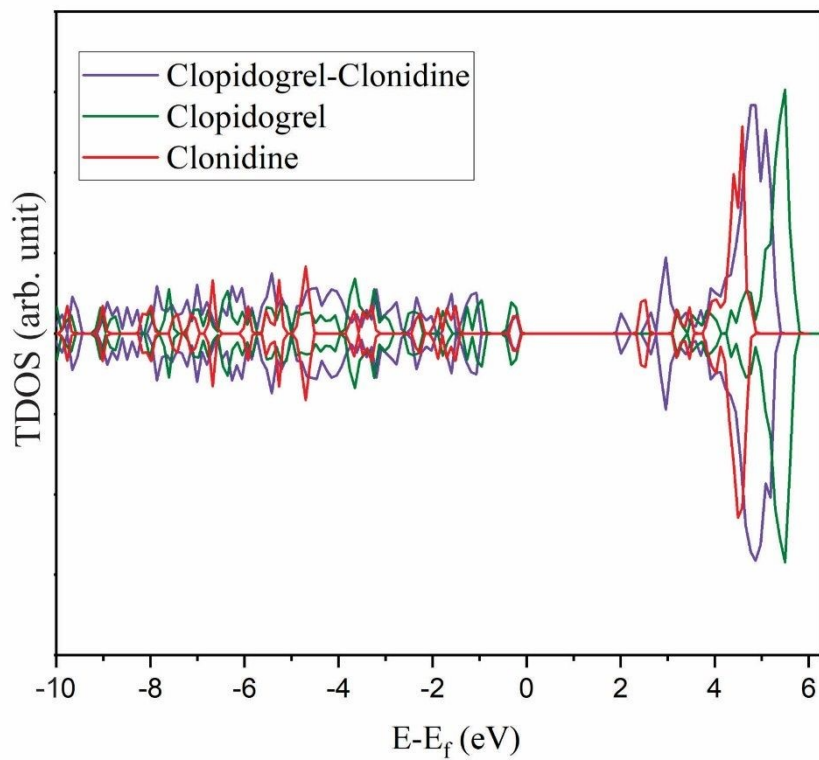


Fig. 6. Total Density of States (TDOS) for clopidogrel-clonidine (C2), isolated clopidogrel and isolated clonidine.



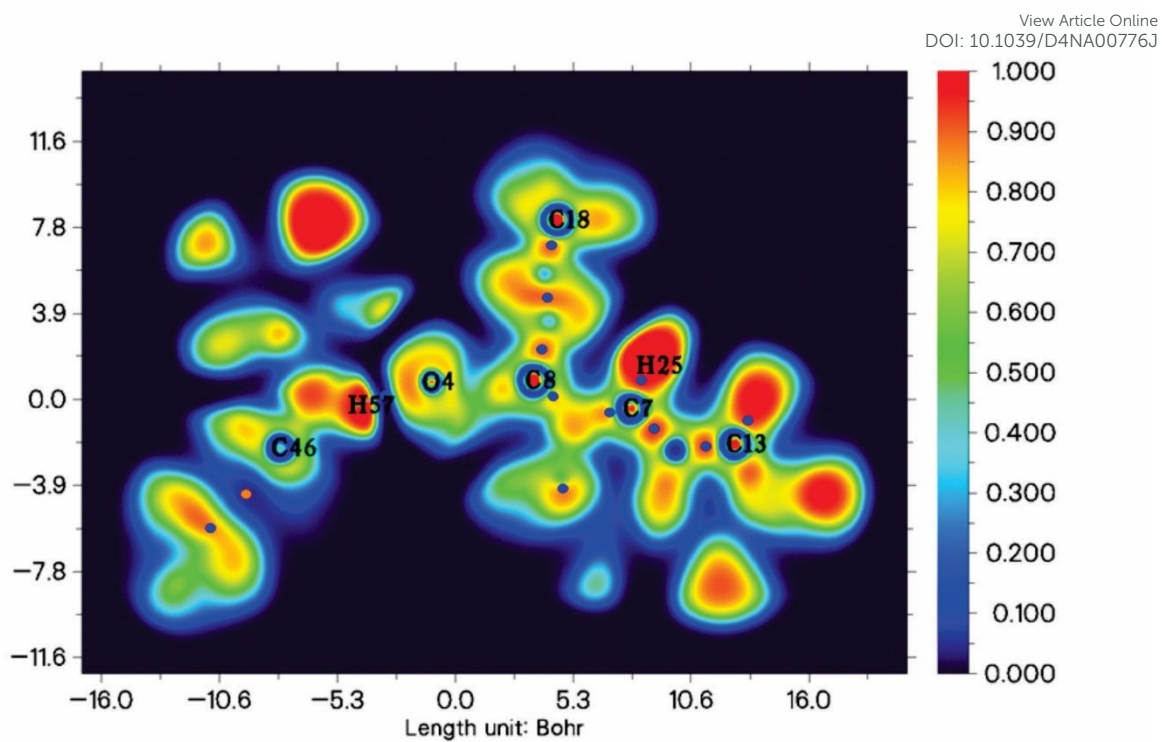


Fig. 7. Electron localization function (ELF) map for clopidogrel-clonidine configuration (C2).



Data for this article are available at **Repositorio Institucional** View Article Online  
DOI: 10.1039/D4NA00776J  
CONICET Digital at <https://ri.conicet.gov.ar/>

Open Access Article. Published on 21 February 2025. Downloaded on 2/22/2025 10:11:14 AM.  
This article is licensed under a Creative Commons Attribution 3.0 Unported Licence.

